World Journal of Engineering and Technology, 2018, 6, 304-314
http://www.scirp.org/journal/wjet
ISSN Online: 2331-4249
ISSN Print: 2331-4222

An Analysis of Double Laplace Equations on a Concave Domain

Hai-Ping Hu

Department of Marine Engineering, National Taiwan Ocean University, Taiwan
Email: hphu@ntou.edu.tw

How to cite this paper: Hu, H.-P. (2018) An Analysis of Double Laplace Equations on a Concave Domain. *World Journal of Engineering and Technology*, **6**, 304-314.
https://doi.org/10.4236/wjet.2018.62019

Received: March 15, 2018
Accepted: May 11, 2018
Published: May 14, 2018

Abstract

In the investigation, the complex geometric domain is a concave geometrical pattern. Due to the symmetric character, the left side of the geometric pattern, *i.e.* the L-shaped region is calculated in the study. The governing equation is expressed with Laplace equations. And the analysis is solved by eigenfunction expansion and point-match method. Besides, visual C^{++} helps obtain the results of numerical calculation. The local values and the mean values of the function are also discussed in this study.

Keywords

Double Laplace Equation, Point-Match

1. Introduction

The Laplace equations show an important role in the applied mathematical researches and analysis. Some significant efforts, thus, have been directed towards researches into related fields. For example, Alliney [1] presented the two-dimensional potential flows to solve the Laplace's equation with appropriate regularity conditions at infinity. The problem is reduced to a finite domain by representing conditions at infinity by means of a boundary integral equation. And Rangogni [2] presented the numerical solution of the generalized Laplace equation by coupling the boundary element method and the perturbation method. Besides, Zanger [3] presented the analysis of the boundary element method applied to Laplace's equation for the experiments involving solving the two-dimensional Laplace problem exterior to a circle and square, using both the direct and indirect methods. Furthermore, Bailey *et al.* [4] presented the generate grid points in two-dimensional simply connected spatial domains. As in many grid generation techniques, the solution of Laplace equation is involved.

And Wang [5] solved the diffusion across a corrugated saw-tooth plate with the Laplace equation. In his study, the transport properties and the theoretical increase in total flux due to corrugations were discussed. Next, Chen *et al.* [6] analyzed the problem of Laplace equation with over-specified boundary conditions. The results show that the unknown boundary potential can be reconstructed, and that both high wave-number content and divergent results can be avoided by using the proposed regularization technique. In addition, L. Gavete *et al.* [7] compared the GFD method with the element free Galerkin method (EFG). The EFG method with linear approximation and penalty functions to treat the essential boundary condition is used in his paper. Both methods are compared for solving Laplace equation. Nyambuya [8] solved the four Poisson-Laplace equations for radial solutions, apart from the Newtonian gravitational component, and obtained four new solutions leading to four new gravitational components capable of explaining e.g. the Pioneer anomaly, the Titius-Bode Law and the formation of planetary rings.

Although many researches about Laplace equation under different conditions have been discussed, the Laplace equation with concave domains is also worth discussing. The present paper, thus, will analyze a symmetric domain with complex Laplace equations under two kinds of boundary conditions in order to find local values and the mean values of the function. The analysis of two kinds of boundary conditions, case 1 and case 2, will be specified in the following mathematical formulation. Furthermore, in the present paper, visualization and image processing are obtained from mathematical formulation of the complex Laplace equations on a concave domain. It is hoped that the results can be further applied in engineering and technology, for example, the problem of fluid flow and heat conduction.

2. Mathematical Formulation

The geometric domain in **Figure 1(a)** is a concave geometric pattern. The outer dimension of the domain is $2w \times h$, and there is a concave, whose dimension is $2(w-d) \times b$. The present research considered two cases of the concave domain. In the first case, the boundary conditions of the bottom is 1, and the boundary conditions of the top is 0. That is to say, the high potential is in the bottom of the domain. And the low potential is in the top of the domain. In the second case, the boundary conditions of the bottom is 0, and the boundary conditions of the top is 1. That is to say, the high potential is in the top of the domain. And the low potential is in the bottom of the domain.

***The analysis of boundary conditions on Case* 1:**

The boundary condition of the bottom is 1, and the condition of the top is 0. The local function distribution in the solid part of the rectangle is $f(x,y)$. Decompose the concave domain into two parts, and due to the symmetric character, only the left hand of the geometry, *i.e.* the L-shaped region in **Figure 1(b)** needs calculating.

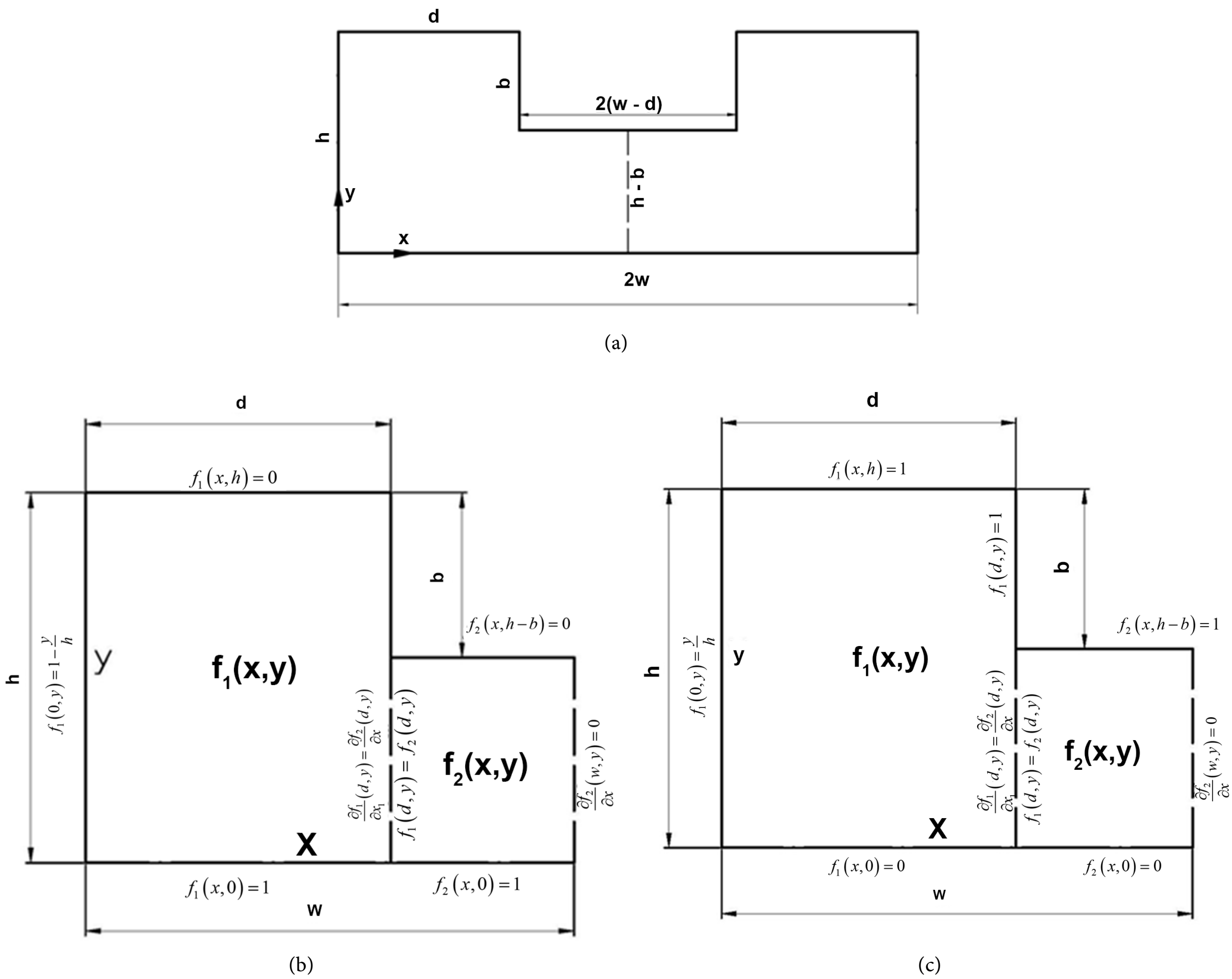

Figure 1. (a) The figure of the concave domain; (b) The geometric pattern for the L-shape domain—Case 1; (c) The geometric pattern for the L-shape domain—Case 2.

The governing equation for the region is expressed with Laplace equation:

$$\nabla^2 f(x,y) = 0 \tag{1}$$

The L-shape region is composed of two rectangles; the governing equation for the left one is:

$$\nabla^2 f_1(x,y) = 0 \tag{2}$$

The boundary conditions for Equation (2) are:

$$f_1(x,0) = 1$$

$$f_1(x,h) = 0$$

$$f_1(0,y) = 1 - \frac{y}{h} \tag{3}$$

And the governing equation for the right rectangle is:

$$\nabla^2 f_2(x,y) = 0 \tag{4}$$

The boundary conditions for Equation (4) are:

$$f_2(x,0)=1$$

$$f_2(x,h-b)=0$$

$$\frac{\partial f_2}{\partial x}(w,y)=0 \tag{5}$$

With the boundary conditions Equations (3) and (5), the analytical solution to Equation (2) is $f_1(x,y)$, and to Equation (6) is $f_2(x,y)$. They are as follows:

$$f_1(x,y)=1-\frac{y}{h}+\sum_n A_n \sin(\alpha_n y)\left(\mathrm{e}^{-\alpha_n(x+d)}-\mathrm{e}^{-\alpha_n(x-d)}\right) \tag{6}$$

$$f_2(x,y)=1-\frac{y}{h-b}+\sum_m B_m \sin(\beta_m y)\left(\mathrm{e}^{\beta_m(x-2w+d)}+\mathrm{e}^{-\beta_m(x-d)}\right) \tag{7}$$

where the eigenvalues are:

$$\alpha=\frac{n\pi}{h}$$

$$\beta=\frac{m\pi}{h-b} \tag{8}$$

Other boundary conditions for governing equations are:

$$f_1(d,y)=0; \qquad h-b\le y\le h \tag{9}$$

We choose N points along the boundary at $x = d$, $y_i = ih/N$ and truncate A_n to N terms and B_m to M terms, where $M=\mathrm{int}\left[(1-b/h)\right]$. Substitute the boundary condition into Equation (6), and the following equation can be obtained:

$$\sum_n A_n \sin(\alpha_n y_i)\left(\mathrm{e}^{-2\alpha d}-1\right)=\frac{y_i}{h}-1 \tag{10}$$

$i = M + 1$ to N

Next, the solutions to the two regions of the L-shape domain can be matched along the common boundary conditions [9]. The conditions can be expressed as:

$$f_1(d,y)=f_2(d,y), \qquad 0\le y<h-b \tag{11}$$

$$\frac{\partial f_1(d,y)}{\partial x}=\frac{\partial f_2(d,y)}{\partial x}, \qquad 0\le y<h-b \tag{12}$$

Substitute the boundary condition into Equations (6)-(7) and can obtain the following equations:

$$\sum_n A_n \sin(\alpha_n y_i)\left(\mathrm{e}^{-2d\alpha}-1\right)-\sum_m B_m \sin(\beta_m y_i)\left(1+\mathrm{e}^{-2(w-d)\beta_m}\right)=\frac{by_i}{h(1-h)} \tag{13}$$

$i = 1$ to M

$$\sum_n A_n\alpha_n \sin(\alpha_n y_i)\left(-1-\mathrm{e}^{-2d\alpha}\right)-\sum_m B_m\beta_m \sin(\beta_m y_i)\left(\mathrm{e}^{-2(w-d)\beta_m}-1\right)=0 \tag{14}$$

$i = 1$ to M

The mean value for $f(x,y)$ is expressed as:

$$f_{mean}=\frac{1}{hw-b(w-d)}\left[\int_0^d\int_0^h f_1\mathrm{d}y\mathrm{d}x+\int_d^w\int_0^{h-b} f_2\mathrm{d}y\mathrm{d}x\right] \tag{15}$$

Integrating Equation (15) can obtain the following equation:

$$\begin{aligned} f_{mean}=\frac{1}{hw-b(w-d)}\Bigg\{&\frac{hw+b(d-w)}{2}+\sum_n\frac{A_n}{\alpha^2}\left(2\mathrm{e}^{-d\alpha}-\mathrm{e}^{-2d\alpha}-1\right)\\ &+\sum_m\frac{B_m}{\beta^2}\left[\cos(h-b)\beta-1\right]\left[\mathrm{e}^{-2\beta(w-d)}-1\right]\Bigg\}\end{aligned} \tag{16}$$

The analysis of boundary conditions on Case **2:**

The geometric domain is also a concave domain. The outer dimension of the domain is $2w\times h$, and there is a concave, whose dimension is $2(w-d)\times b$. The boundary condition of the bottom is 0, and the condition of the top is 1. The L-shape region, in **Figure 1(c)** is composed of two rectangles.

The governing equation for the left rectangle is:

$$\nabla^2 f_1(x,y)=0 \tag{17}$$

The boundary conditions for Equation (17) are:

$$f_1(x,0)=0$$
$$f_1(x,h)=1$$
$$f_1(0,y)=\frac{y}{h} \tag{18}$$

And the governing equation for the right rectangle is:

$$\nabla^2 f_2(x,y)=0 \tag{19}$$

The boundary conditions for Equation (19) are:

$$f_2(x,0)=0$$
$$f_2(x,h-b)=1$$
$$\frac{\partial f_2}{\partial x}(w,y)=0 \tag{20}$$

With the boundary conditions Equations (18) and (20), the analytical solution to Equation (17) is $f_1(x,y)$, and to Equation (19) is $f_2(x,y)$. They are as follows:

$$f_1(x,y)=\frac{y}{h}+\sum_n C_n\sin(\alpha_n y)\left(\mathrm{e}^{-\alpha_n(x+d)}-\mathrm{e}^{-\alpha_n(x-d)}\right) \tag{21}$$

$$f_2(x,y)=\frac{y}{h-b}+\sum_m D_m\sin(\beta_m y)\left(\mathrm{e}^{\beta_m(x-2w+d)}+\mathrm{e}^{-\beta_m(x-d)}\right) \tag{22}$$

where the eigenvalues are:

$$\alpha=\frac{n\pi}{h}$$
$$\beta=\frac{m\pi}{h-b} \tag{23}$$

Other boundary conditions for governing equations are:

$$f_1(d,y)=1; \qquad h-b\le y\le h \tag{24}$$

Substitute the boundary condition into Equation (21), and the following equation can be obtained:

$$\sum_n C_n \sin(\alpha_n y_i)\left(1-\mathrm{e}^{-2\alpha d}\right)=1-\frac{y}{h} \tag{25}$$

$i = M + 1$ to N

Next, the solutions to the two regions of the L-shape domain can be matched along the common boundary conditions. The conditions can be expressed as:

$$f_1(d,y)=f_2(d,y), \qquad 0\le y<h-b \tag{26}$$

$$\frac{\partial f_1(d,y)}{\partial x}=\frac{\partial f_2(d,y)}{\partial x}, \qquad 0\le y<h-b \tag{27}$$

Substitute the boundary condition into Equations (21)-(22), and can obtain the following equations:

$$\sum_n C_n \sin(\alpha_n y_i)\left(\mathrm{e}^{-2d\alpha}-1\right)-\sum_m D_m \sin(\beta_m y_i)\left(1+\mathrm{e}^{-2(w-d)\beta_m}\right)=\frac{by_i}{h(h-b)} \tag{28}$$

$i = 1$ to M

$$\sum_n C_n\alpha_n \sin(\alpha_n y_i)\left(-1-\mathrm{e}^{-2d\alpha)}\right)-\sum_m D_m\beta_m \sin(\beta_m y_i)\left(\mathrm{e}^{-2(w-d)\beta_m}-1\right)=0 \tag{29}$$

$i = 1$ to M

The mean value for $f(x,y)$ is expressed as:

$$f_{mean}=\frac{1}{hw-b(w-d)}\left[\int_0^d\int_0^h f_1\mathrm{d}y\mathrm{d}x+\int_d^w\int_0^{h-b} f_2\mathrm{d}y\mathrm{d}x\right] \tag{30}$$

Integrating Equation (30) can obtain the following equation:

$$\begin{aligned}f_{mean}=\frac{1}{hw-b(w-d)}&\left\{\frac{hw+b(d-w)}{2}+\sum_n\frac{C_n}{\alpha^2}\left(2\mathrm{e}^{-d\alpha}-\mathrm{e}^{-2d\alpha}-1\right)\right.\\&\left.+\sum_m\frac{D_m}{\beta^2}\left[\cos(h-b)\beta-1\right]\left[\mathrm{e}^{-2\beta(w-d)}-1\right]\right\}\end{aligned} \tag{31}$$

3. Numerical Methods

The following steps of numerical methods are estimated by using Visual C++:

1) Give the constants h, b, w and d.

2) Set $N = 29$, $M=\mathrm{int}\left[(1-b/h)\right]$ and $y_i=ih/N$, $1\le i\le N$.

3) Equations (10), (13) and (14) are expressed as the linear system of ($N + M$) equations to solve coefficients A_n and B_m.

4) Substitute coefficients A_n and B_m into equations f_1, (Equation (6)) and f_2 (Equation (7)). This process is repeated at all nodes within the range, *i.e.* $0\le y\le h$, $0\le x\le w$.

5) Map the $f(x,y)$ on the entire domain.

6) The average values of function can be calculated from Equation (16).

7) Repeat the previous methods can estimate the results of Case 2.

4. Results and Discussion

Results and discussion of Case **1:**

Figure 2(a) and Figure 2(b) show the contour plot for the domain. Figure 2(a) is a concave ($2w = 1.0$, $h = 0.5$). In the figures, *w*, *b*, *h* and *d* values are different. With the boundary condition Equations (3), (5) and governing equation $f_1(x,y)$ and $f_2(x,y)$, the function values distributing from the bottom of the domain, $f = 1.0$ to the top, $f = 0$ gradually decrease. Besides, the bottom of the domain is high potential, e. g. high temperature or high pressure. The top of the concave domain is low potential, e.g. low temperature or low pressure. The figures show the function values distributing from the maximum value of the bottom to the minimum value of the top gradually decrease.

Figure 2(c) shows the local function values for the entire domain ($x = 0$ to $x = 2w$, $y = 0$ to $y = h$). As the figure shows, the bottom region has the maximum function values, *i.e.* $f = 1.0$, and then function values gradually decrease from the bottom to the top of the concave domain, $f = 0$.

Figure 3 shows the influence of h on the mean values of $f(x,y)$ under three different *b* values ($b = 0.25$, 0.35 and 0.45). According to Equation (16), the larger values of the depth of the concave domain *b*, and the height of the concave

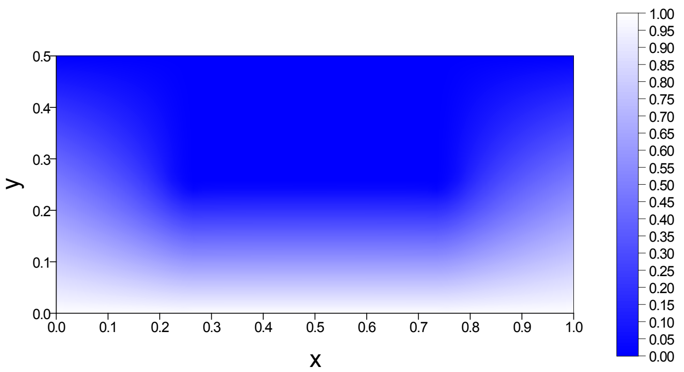

(a)

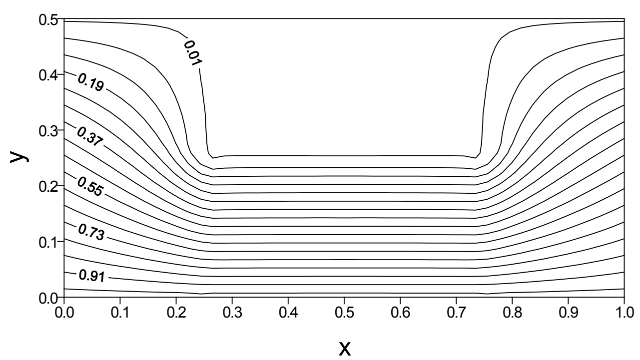

(b)

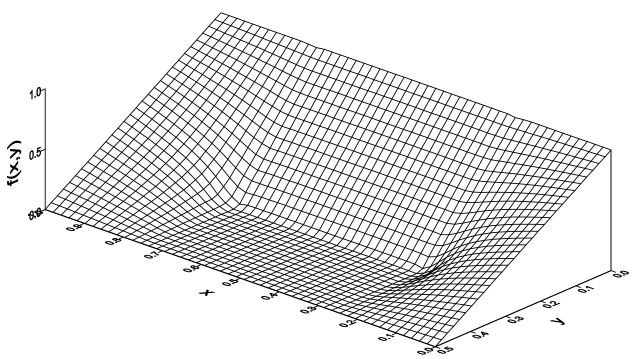

(c)

Figure 2. (a) Image for function values, $h = 0.5$, $b = 0.25$, $d = 0.25$, $2w = 1.0$; (b) Contour plot for function values, $h = 0.5$, $b = 0.25$, $d = 0.25$, $2w = 1.0$; (c) The distribution of local function values, $h = 0.5$, $b = 0.25$, $d = 0.25$, $2w = 1.0$.

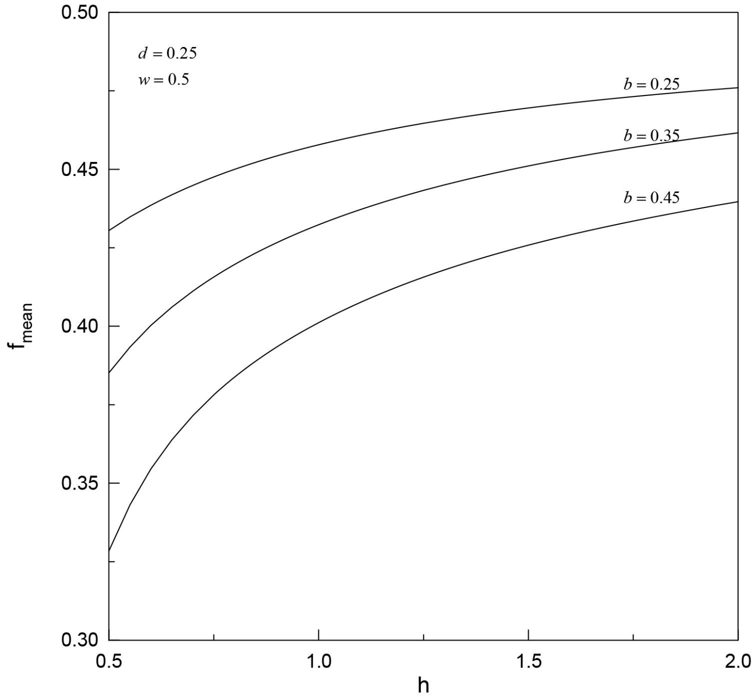

Figure 3. Mean function values for $w = 0.5$, $d = 0.25$—effect on values of h.

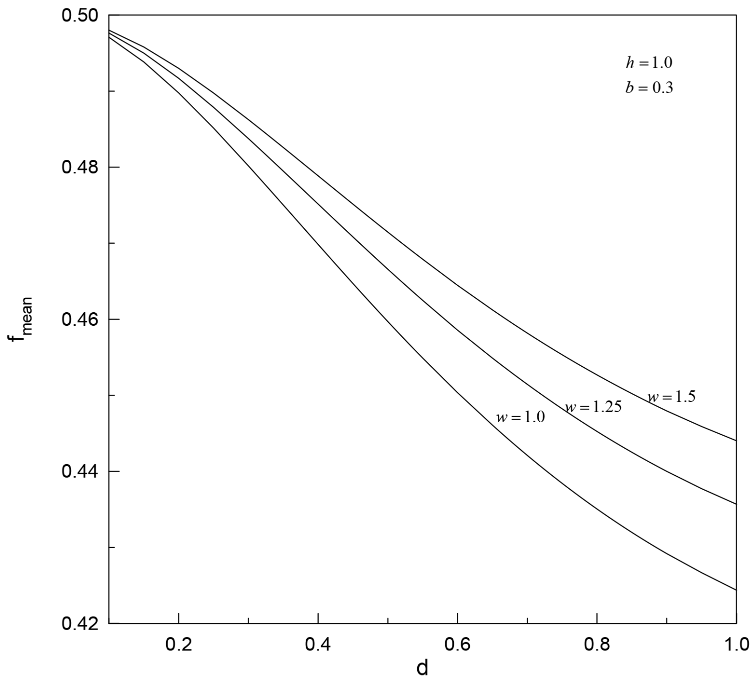

Figure 4. Mean function values for $h = 1.0$, $d = 0.3$—effect on values of d.

domain h will influence the coefficient A_n and B_m, and then the mean values of f_{mean} will increase. As the figure shows, from $h = 0.5$ to $h = 2.0$, the mean values of function $f(x, y)$ increase from $h = 0.5$, and then the mean values gradually increase to $h = 2.0$. Thus, under the particular range of the height and the width, the larger the high values of domain h will bring the larger mean values.

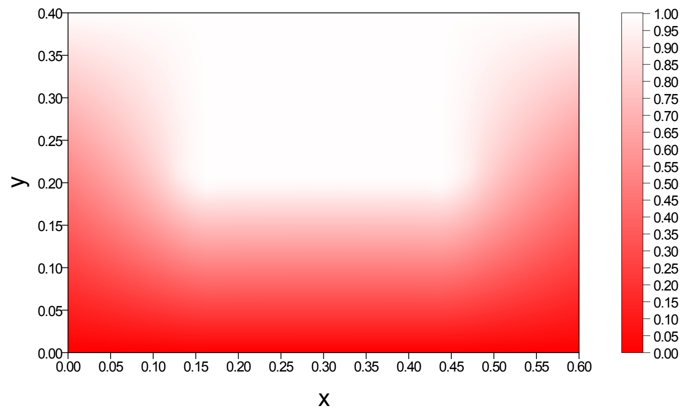

(a)

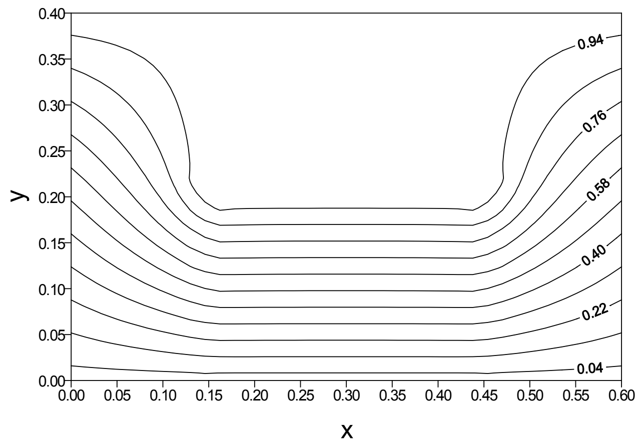

(b)

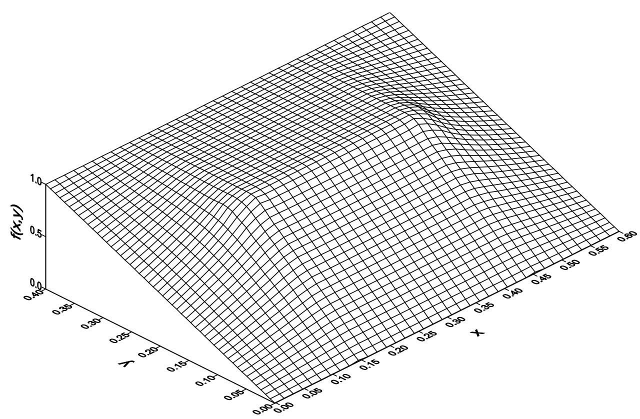

(c)

Figure 5. (a) Image for function values, $h = 0.4$, $b = 0.2$, $d = 0.15$, $2w = 0.6$; (b) Contour plot for function values, $h = 0.4$, $b = 0.2$, $d = 0.15$, $2w = 0.6$; (c) The distribution of local function values for $h = 0.4$, $b = 0.2$, $d = 0.15$, $2w = 0.6$.

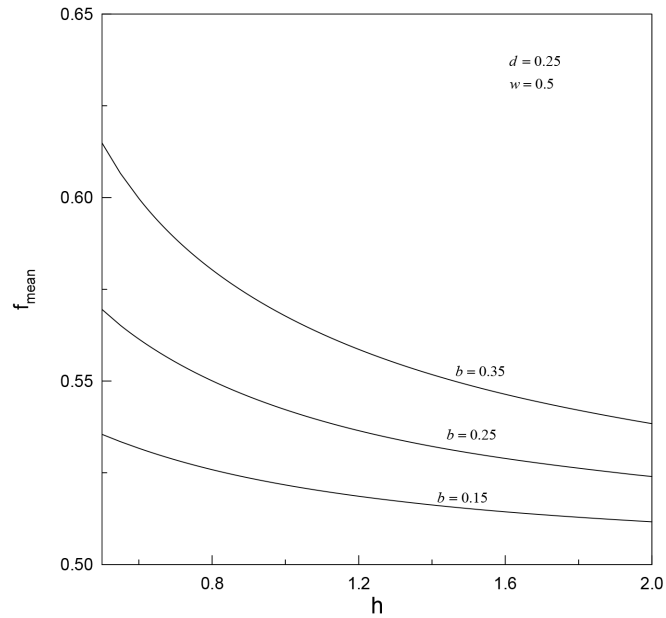

Figure 6. Mean function values for $w = 0.5$, $d = 0.25$—effect on values of h.

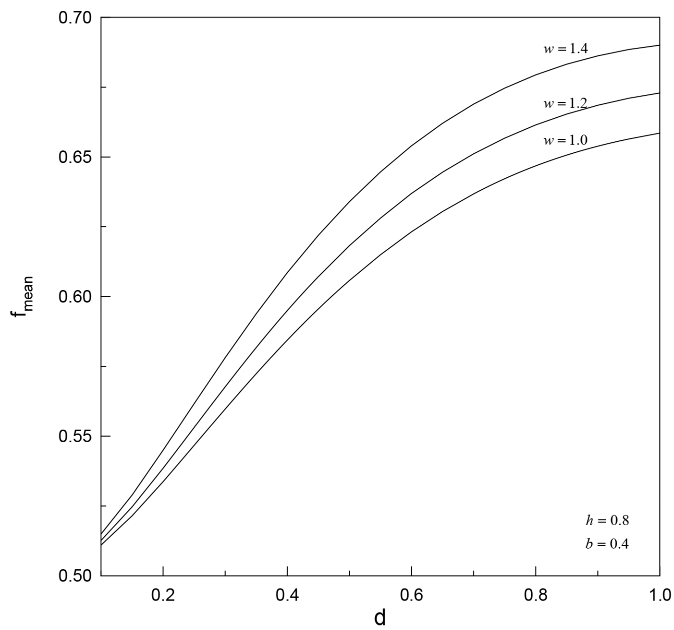

Figure 7. Mean function values for $h = 0.8$, $d = 0.8$—effect on values of d.

Figure 4 shows the influence of the values d on the mean values of $f(x, y)$ under three different w values. According to Equations (6), (7) and (16), the larger values of the width of the concave domain w, and the width of the left-top of the concave domain d will also influence the coefficient A_n and B_m, and then the mean values of f_{mean} will increase. Besides, observation of the figure shows that the mean values decrease as the values of d increase. And the increase in w leads to an increase in the mean values.

***Results and* discussions *of Case* 2:**

Figure 5(a) and **Figure 5(b)** show the contour plot for the concave domain ($2w = 0.6$, $h = 0.4$). Basing on the boundary conditions of the case, the function values distributing from the bottom of the domain, $f = 0$ to the top of the domain, $f = 1.0$ gradually increase.

Figure 5(c) shows the local function values for the entire domain ($x = 0$ to $x = 2w$, $y = 0$ to $y = h$). As the figure shows, the lower region has the minimum function values, *i.e.* $f = 0$, and then function values gradually increase from bottom to the top of the concave, $f = 1.0$.

Figure 6 shows the influence of h on the mean values of $f(x, y)$ under three different b values. As the figure shows, from $h = 0.5$ to $h = 2.0$, the mean values of function $f(x, y)$ decrease from $h = 0.5$ to $h = 2.0$.

Figure 7 shows the influence of the values d on the mean values of $f(x, y)$ under three different w values ($w = 1.0$, 1.2 and 1.4). Observation of the figure shows that the mean values increase as the values of d increase. And the increase in w leads to an increase in the mean values.

5. Conclusion

The present paper can find the influence of the height and the width of the geometric domain on the function mean values. Besides, the present paper uses the analytical solution of point match methods and numerical methods which can easily compute coefficient A_n, B_m, C_n, D_m and function $f(x, y)$.

Acknowledgements

The authors gratefully acknowledge the support provided to this projects by the Ministry of Science and Technology of the Taiwan under Contract Number MOST 106-2221-E-019-062.

References

[1] Alliney, S. (1982) A Numerical Study of Two Dimensional Potential Flows by Boundary and Finite Elements. *Applied Mathematical Modelling*, **6**, 291-298. https://doi.org/10.1016/S0307-904X(82)80037-1

[2] Rangogni, R. (1986) Numerical Solution of the Generalized Laplace Equation by Coupling the Boundary Element Method and the Perturbation Method. *Applied Mathematical Modelling*, **10**, 266-270. https://doi.org/10.1016/0307-904X(86)90057-0

[3] Kirkup, S.M. and Henwood, D.J. (1994) An Empirical Error Analysis of the Boundary Element Method Applied to Laplace's Equation. *Applied Mathematical Modelling*, **18**, 32-38. https://doi.org/10.1016/0307-904X(94)90180-5

[4] Bailey, R.T., Hsieh, C.K. and Li, H. (1995) Grid Generation in Two Dimensions Using the Complex Variable Boundary Element Method. *Applied Mathematical Modelling*, **19**, 322-332. https://doi.org/10.1016/0307-904X(95)00008-8

[5] Wang, C.Y. (1994) Diffusion across a Corrugated Saw-Tooth Plate. *Mechanics Research Communications*, **116**, 233-237.

[6] Chen, J.T. and Chen, K.H. (1998) Analytical Study and Numerical Experiments for Laplace Equation with Overspecified Boundary Conditions. *Applied Mathematical Modelling*, **22**, 703-725. https://doi.org/10.1016/S0307-904X(98)10054-9

[7] Gavete, L., Gavete, M.L. and Benito, J.J. (2003) Improvements of Generalized Finite Difference Method and Comparison with Other Meshless Method. *Applied Mathematical Modelling*, **27**, 831-847. https://doi.org/10.1016/S0307-904X(03)00091-X

[8] Nyambuya, G.G. (2015) Four Poisson-Laplace Theory of Gravitation (I). *Journal of Modern Physics*, **6**, Article ID: 58605, 11 p.

[9] Hu, H.P. (2015) The Two-Dimensional Analysis of Laminar Flow Between the Moving Plates with Arrayed Rods. *Journal of the Chinese Society of Mechanical Engineers*, **4**, 317-322.